DENTAL MATERIALS 25 (2009) 103–114

available at www.sciencedirect.com

ScienceDirect

journal homepage: www.intl.elsevierhealth.com/journals/dema

Influence of thermal expansion on shrinkage during photopolymerization of dental resins based on bis-GMA/TEGDMA

Veronica Mucci[a], *Gustavo Arenas*[b], *Ricardo Duchowicz*[c], *Wayne D. Cook*[d], *Claudia Vallo*[a,*]

[a] *Instituto de Investigación en Ciencia y Tecnología de Materiales (INTEMA), Mar del Plata, Argentina*
[b] *Facultad de Ingeniería, Universidad Nacional de Mar del Plata (UNMdP), Argentina*
[c] *Centro de Investigaciones Opticas (CIOp) y Facultad de Ingeniería (UNLP), Argentina*
[d] *Department of Materials Engineering, Monash University, Melbourne, Victoria, Australia*

ARTICLE INFO

Article history:
Received 2 October 2007
Accepted 15 April 2008

Keywords:
Dental resins
Dimethacrylates
Photopolymerization
Polymerization shrinkage
Interferometric method
Exotherm

ABSTRACT

Objective. The aim of this study was to assess volume changes that occur during photopolymerization of unfilled dental resins based on bis-GMA-TEGDMA.

Methods. The resins were activated for visible light polymerization by the addition of camphorquinone (CQ) in combination with dimethylamino ethylmethacrylate (DMAEMA) or ethyl-4-dimethyl aminobenzoate (EDMAB). A fibre-optic sensing method based on a Fizeau-type interferometric scheme was employed for monitoring contraction during photopolymerization. Measurements were carried out on 10 mm diameter specimens of different thicknesses (1 and 2 mm).

Results. The high exothermic nature of the polymerization resulted in volume expansion during the heating, and this effect was more pronounced when the sample thickness increased. Two approaches to assess volume changes due to thermal effects are presented. Due to the difference in thermal expansion coefficients between the rubbery and glassy resins, the increase of volume due to thermal expansion was greater than the decrease in volume due to thermal contraction. As a result, the volume of the vitrified resins was greater than that calculated from polymerization contraction. The observed trends of shrinkage versus sample thickness are explained in terms of light attenuation across the path length during photopolymerization.

Significance. Results obtained in this research highlight the inherent interlinking of non-isothermal photopolymerization and volumetric changes in bulk polymerizing systems.

1. Introduction

Photocuring of multifunctional monomers is a well-known method applied in clinical restorative dentistry. The major disadvantage of dental composites over amalgam is that they shrink during polymerization causing shrinkage strain and marginal gaps at the tooth composite interface. [1,2] Therefore, the reduction of composite shrinkage presents an important goal in biomaterials research.

It is well known that the exothermic nature of free radical bulk polymerization of dimethacrylate monomers leads to elevated cure temperatures. Consequently, the shrinkage

* *Corresponding author at*: Avenue Juan B. Justo 4302, (7600) Mar del Plata, Argentina.
E-mail address: civallo@fi.mdp.edu.ar (C. Vallo) .

0109-5641/$ – see front matter © 2008 Academy of Dental Materials. Published by Elsevier Ltd. All rights reserved.
doi:10.1016/j.dental.2008.04.014

that occurs due to the polymerization reaction is accompanied with volumetric expansions and contractions resulting from the temperature changes. In highly filled resin composites, the temperature increase is partly reduced by the presence of the filler. However, for less highly filled composites (e.g. marginal sealants) and for experimental studies of polymeric shrinkage of unfilled resins, the thermal effects during polymerization must be taken into account. The present study has been conducted to gain a further insight into the volumetric changes which occur during photopolymerization under non-isothermal conditions.

Several methods for the measurement of shrinkage in dental composites have been proposed. The methods are based on two general approaches: volume dilatometry or non-volume dilatometric methods. The change in density and volume of the composite has been assessed by dilatometry [3–5] or gas pycnometry. [6] Non-volume dilatometric measurements are usually one-dimensional and employ a contacting or non-contacting transducer including the linometer [7,8], the bonded-disk technique [9], thermomechanical analysis [10], and optical methods [11–14]. In this study, a non-contact, Fizeau-type interferometric method for monitoring the shrinkage development during photopolymerization of unfilled dental resins was employed. The technique enables quantitative measurements providing data for the continuous shrinkage evolution during photopolymerization. The ability to collect data at high acquisition rates permits the real-time monitoring of extremely fast chemical reactions as in the case of the polymerization of multifunctional methacrylate monomers.

Two approaches to predict the volume changes that occur during photopolymerization, including both thermal effects and polymerization effects are presented. Computations were carried out by combining experimental measurements of shrinkage evolution, double bond conversion and temperature profiles during photopolymerization. Results obtained in this research highlight the inherent interlinking of non-isothermal photopolymerization and volumetric changes in bulk polymerizing systems.

2. Materials and methods

2.1. Materials

The resins were formulated from blends of {2,2-bis[4-(2-hydroxy-3-methacryloxyprop-1-oxy)phenyl]propane} (bis-GMA) and triethylene glycol dimethacrylate (TEGDMA) at mass fractions 70:30 bis-GMA/TEGDMA. bis-GMA (Esstech, Essington, PA, USA) and TEGDMA (Aldrich) were used as received. The resins were activated for visible light polymerization by the addition of camphorquinone (CQ) and amine reducing agents. The amines were dimethylaminoethylmethacrylate (DMAEMA) (Aldrich) and ethyl-4-dimethylaminobenzoate (EDMAB) (Aldrich). The structure of the monomers and photoinitiator systems are depicted in Scheme 1.

2.2. Light source

The light source employed to cure the resins was assembled from a Light Emitting Diode (LED, OTLH-0090-BU, Optotech Inc.), with its emittance centered at 470 nm. The LED was selected taking into account that the CQ photoactivator is activated in the wavelength range 400–500 nm with an absorption peak at 470 nm. The emission spectrum of the LED source was

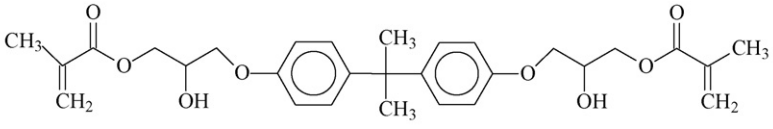

Bis-GMA

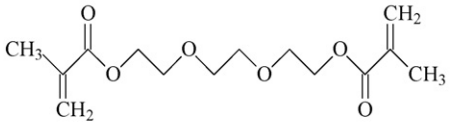

TEGDMA

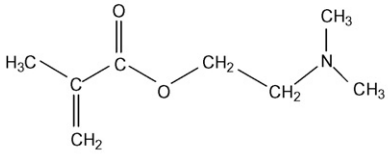

DMAEMA

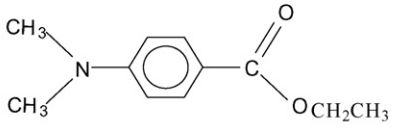

EDMAB

Scheme 1 – Molecular structure of the monomers and photoinitiators.

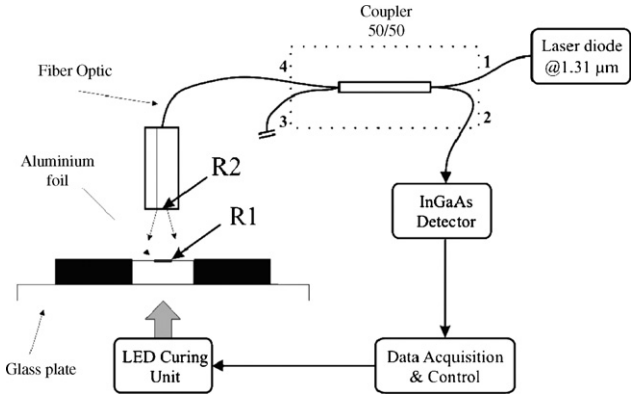

Fig. 1 – Schematic diagram of the interferometer apparatus. All components are mounted on a vibration isolation optical table.

measured with a calibrated CVI-monochromator (Digikrom 480) and a Si-photodetector. The power of the photocuring source was measured with a calibrated laser probe thermopile sensor. The irradiance of the source at the base of the polymerizing specimen was measured to be 30 mW.

2.3. *Measurement of volumetric shrinkage*

A fibre optic sensing method based on a Fizeau-type interferometric scheme was employed for monitoring the evolution of the shrinkage during photopolymerization. Details of the technique were reported elsewhere [14] and are briefly described here. Fig. 1 depicts the experimental arrangement. A laser diode operating at 1.31 μm was used as the coherent source of the interferometer (Mitsubishi 725B8F mounted on Thorlabs KT112 collimation and focusing system, powered with LD2000 Thorlabs Laser Driver). Laser light was coupled to a 2 × 2 single mode (1.31 μm) fiber directional coupler (Thorlabs 10202A-50). Two optical waves are coupled back into the fiber from the Fizeau interferometer. The optical signal from one of the outputs (labelled as 2 in Fig. 1) was collected by an InGaAs detector (Thorlabs DET410), amplified, converted to a digital signal and acquired on a PC (personal computer) at 500 samples/s. A further averaging process was performed before plotting the values. In order to avoid spurious signals, light reflections from another output of the coupler (labelled as 3 in Fig. 1) were eliminated by the employment of an index adapter liquid. An air-gap was developed between the cleaved end (corresponding to the output labelled as 4 in Fig. 1) of the single mode directional coupler (reflectance labelled as R2 in Fig. 1) and a reflective surface consisting of a very small piece (1 mm × 1 mm) of thin aluminium foil was placed onto the resin sample (reflectance labelled as R1 in Fig. 1). The glass plate was fixed to a positioning system which was aligned in order to ensure that the two reflective planes R1 and R2 were parallel. Beams coming from R1 and R2 interfere and, if the distance between both reflective surfaces changes, the coherent process generates a temporal modulation (intensity distribution of maxima and minima. Thus, the separation between two intensity maxima corresponding to two consecutive interference fringes occurs at $\Delta L = \lambda/2$ or 0.655 μm [14]. Mechanical vibrations give rise to noise that complicate contraction measurements, so it is important to assemble the apparatus in a vibration free environment. The apparatus used in the present experiment was assembled on a vibration free optical table.

A rubber ring of inner diameter equal to 10 mm was glued to the microscope glass plate. The sample resin was placed onto the glass plate in the centre of the rubber ring and the small piece (1 mm × 1 mm) of reflective thin aluminium paper was placed on top of the sample. The fibre end was aligned parallel to the reflective foil with an initial separation of less than 100 μm. When the system was stabilized and a nearly continuous optical signal of 1.31 μm reflected from the interferometer was observed on the oscilloscope, data acquisition commenced five seconds before the LED was turned on, and thus, the optical signal was acquired and processed. For each signal point plotted, three experimental data were averaged. Measurements were carried out on samples of 1 and 2 mm thickness. The samples were recovered at the conclusion of each experimental run by using a razor blade to remove them from the microscope slide. The sample thickness was then measured to within ±2% with a precision micrometer. The initial sample thickness, L_0, was calculated as the sum of the thickness measured immediately after the test and the total ΔL measured from the interferogram register. The samples were irradiated for 320 s and data acquisition continued with the LED unit turned off to complete the 600 s experimental period.

2.4. *Measurement of temperature evolution during photopolymerization*

The temperature during polymerization was monitored in specimens of the same thickness to those used in the shrinkage measurements (1 and 2 mm), with fine K-type thermocouples (Omega Engineering Inc., USA) embedded in the resin. The thermocouples were connected to a data acquisition system that registered values of temperature every 1 s. The samples were irradiated for 320 s and the data acquisition continued with the LED unit turned off to complete the 600 s experimental period. Three replicates were conducted for each experiment. The experimental conditions, i.e. glass plate support, rubber ring and irradiation method, were the same as those for the shrinkage measurements. This ensured that the heat transfer of the different tests was the same.

2.5. *Measurement of the coefficient of thermal expansion*

Measurements of changes in the volume of the monomer and vitrified resins versus temperature were performed during cooling of the samples. A sample was placed onto a thermostated heating plate and its temperature recorded once every second. When the sample reached a steady temperature, the thermostat was turned off and the temperature and volume were simultaneously monitored during the cooling period. Samples of monomer were cooled from 90 to 25 °C at a cooling rate of 2.92 °C/min whereas samples of glassy resins were cooled from 45 to 20 °C at an average cooling rate of 1.2 °C/min. The coefficient of thermal expansion was calculated from the resulting linear plots of ΔV versus ΔT, where

ΔV is the decrease in volume measured by the interferometer and ΔT is the temperature decrease measured with the thermocouple embedded in the sample.

2.6. Measurement of the specific heat

The specific heat measurements of monomer and photopolymerized samples were made with a Shimadzu TA 50 calorimeter provided with software which enables processing of the data generated by each run. Calibrations were made with high purity alumina.

2.7. Measurement of double bond conversion

FTIR spectra were acquired with a Genesis II Mattson FT-IR (Madison, WI, USA). NIR spectra were acquired over the range 4500–7000 cm^{-1} [15] from 16 co-added scans at 2 cm^{-1} resolution. The co-added spectra took 120 s to acquire. Unfilled resins were sandwiched between two glass plates separated by a 2 mm thick rubber spacer, and were tightly attached to the sample holder using small clamps. With the assembly positioned in a vertical position, the light source was placed in contact with the glass surface. In order to obtain the double bond conversion as a function of the irradiation time, different samples were irradiated for 5, 10, 20, 40, 60, 80 and 100 s. Spectra were collected 120 s after the exposure interval. The background spectrum was collected through an empty mold assembly fitted with only one glass slide to avoid internal reflectance patterns. The conversion profiles were calculated from the decay of the absorption band located at 6165 cm^{-1}. Three replicates were used in the measurement of conversion.

2.8. Measurement of the molar extinction coefficient of CQ

The UV absorption spectra of CQ was measured with an UV–vis spectrophotometer 1601PC Shimadzu in 10 mm cuvettes using ethanol as solvent. The concentration of CQ was 3.65×10^{-3} mol/L.

3. Results and discussion

Fig. 2 shows a typical interferogram. When the sample is irradiated, the polymerization proceeds with its associated contraction. As the sample thickness decreases the distance between both reflective surfaces (ΔL) increases and a very clear intensity pattern is observed with a resolution less than 0.1 μm. Polymerization shrinkage is a multiaxial phenomenon. The compensation for shrinkage at free borders makes it difficult to record volumetric shrinkage from measurements along only one axis. However if the lateral shrinkage of the specimen can be restrained by bonding to the substrate then the vertical shrinkage is equal to the volumetric shrinkage. This lateral restraint can be achieved, subject to three conditions—the resin must be in the gelled state so that flow does not occur, the gel must be bonded to the substrate and the specimen must have a squat shape so that lateral shrinkage of its free surface is constrained by the bonded surface. It is well known that dimethacrylates gel at low

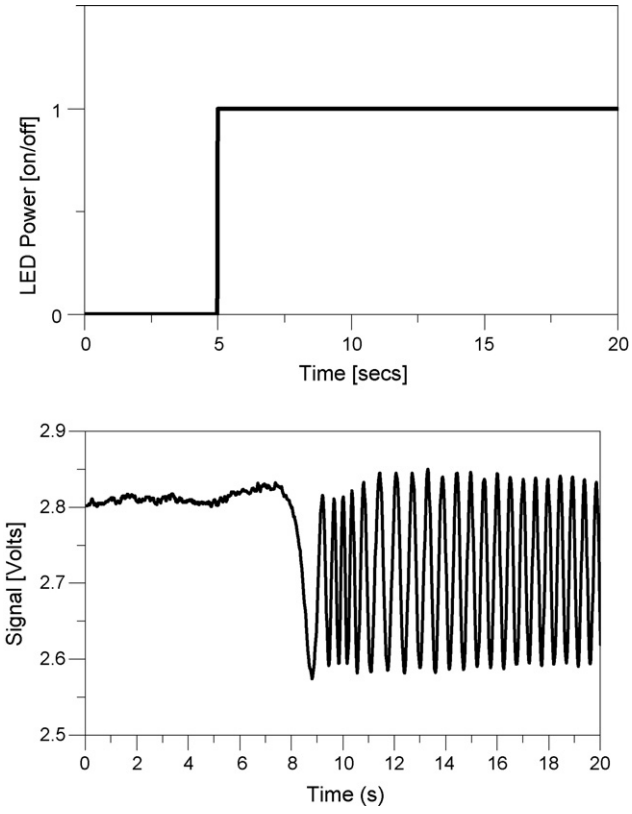

Fig. 2 – Typical interferogram collected from the detector. The cure light was turned on at 5 s.

conversions (typically less than 1%) so that the first condition is fulfilled. The specimen geometry (1 or 2 mm high and 10 mm diameter) was chosen (Fig. 1) so that the specimen adhered to the glass substrate (as noted above) and so that the specimen aspect ratio (diameter/thickness) was sufficiently high for the lateral boundary effects to be minimized [16,17]. Therefore, the percent of volumetric contraction can be calculated by the following expression:

$$\text{Shrinkage} = 100\frac{\Delta V}{V_0} \approx 100\frac{\Delta L}{L_0} \quad (1)$$

Fig. 3a and b shows the shrinkage over time during photopolymerization for formulations prepared with 1 wt.% CQ in combination with an equimolar proportion of EDMAB or DMAEMA. Significant differences in the rate of contraction were measured between resins containing these amines. EDMAB, is a very effective hydrogen donor and rapid cures are obtained even at low accelerator concentrations [18,19]. Conversely, DMAEMA is a less efficient photoreducer resulting in low polymerization rate and lower conversion compared with the EDMAB aromatic amine [18,19]. The values of volumetric shrinkage are much higher than those reported for commercial dental dimethacrylate composites, because the latter are filled with non-shrinking inorganic particles. The contraction started after an induction time, which was obtained from the data as the time that transpired between the start of irradiation and the beginning of oscillations in the sample interfer-

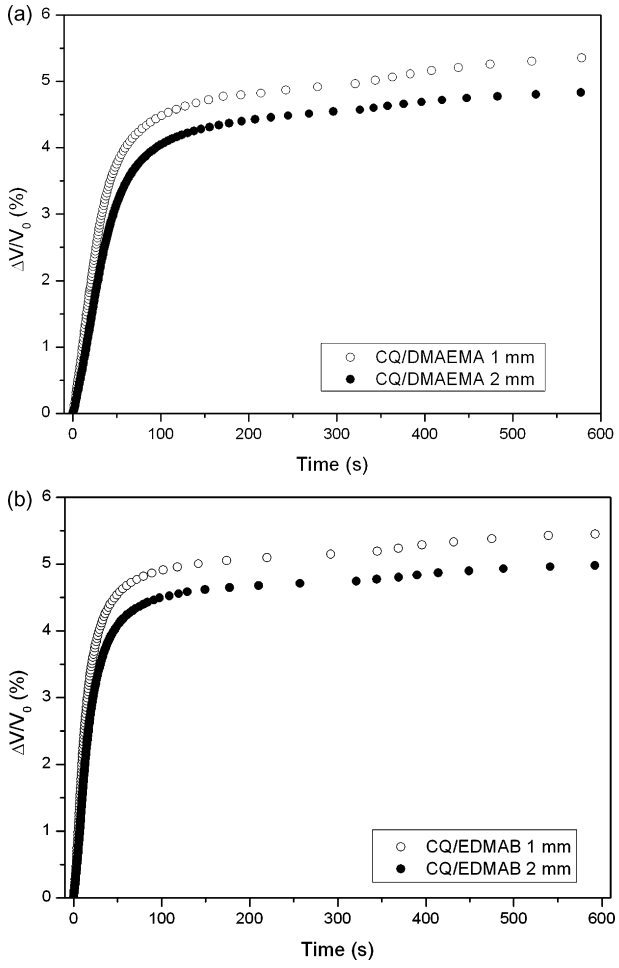

Fig. 3 – (a) Shrinkage vs. time during photopolymerization for formulations containing 1 wt.% CQ/DMAEMA and different sample thickness. The LED unit was turned off at 320 s. (b) Shrinkage vs. time during photopolymerization for formulations containing 1 wt.% CQ/EDMAB and different sample thickness. The LED unit was turned off at 320 s.

ogram. This time lag at the beginning of each shrinkage profile is attributed to the presence of both free radical inhibitor in the resin and dissolved oxygen. According to the manufacturers, the bis-GMA resin contains 570 ppm of methoxyhydroquinone (MEHQ) to inhibit self-polymerization during storage and it was used as received without further purification. In addition, the resins were not degassed before the experiment commenced and so a significant amount of oxygen was dissolved in the resin. Furthermore, the top surface of the test sample was exposed to air during the course of the measurements, allowing oxygen flux into the resins. The mechanisms of oxygen inhibition have been the subject of several previous investigations [20–24]. Oxygen is known to inhibit free radical polymerizations by reacting with initiator, primary, and growing polymer radicals to form peroxy radicals. The peroxy radicals are more stable and do not readily reinitiate polymerization, and thus, the oxygen essentially terminates or consumes radicals. The atmospheric oxygen and MEHQ inhibit photopolymerization by scavenging initiator radicals and so competing with the reaction between initiator radicals and monomer. Consequently, the photocuring reaction is delayed until nearly all the inhibitor or oxygen is consumed. Another variable that dramatically affects the extent of oxygen inhibition of free radical photopolymerization is the initiation rate. If the initiation rate (determined by the initiator concentration and activity and the radiation intensity) is sufficiently low, all of the radicals generated could be consumed in the inhibition process. Thus formulations prepared with the more reactive photoinitiator system (CQ/EDMAB) resulted in the lowest induction period because the inhibiting species were consumed faster.

It is well known that the dimethacrylates polymerization reaction is highly exothermic. Thus, the temperature of the sample during polymerization is expected to increase. Fig. 4a and b shows the temperature profiles measured during resin photopolymeration under identical conditions to those used in shrinkage measurements. Samples containing CQ/EDMAB exhibited a maximum increase in temperature of 20 and 30 °C while for samples containing CQ/DMAEMA the maximum

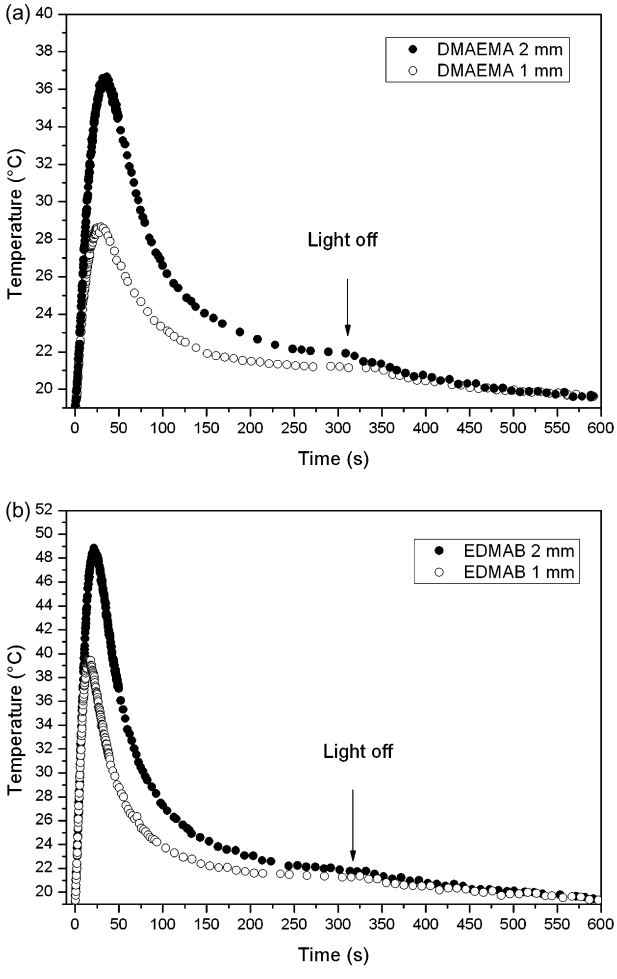

Fig. 4 – (a) Temperature evolution during the photopolymerization of samples containing 1 wt.% CQ/DMAEMA. The LED unit was turned off at 320 s. (b) Temperature evolution during the photopolymerization of samples containing 1 wt.% CQ/EDMA. The LED unit was turned off at 320 s.

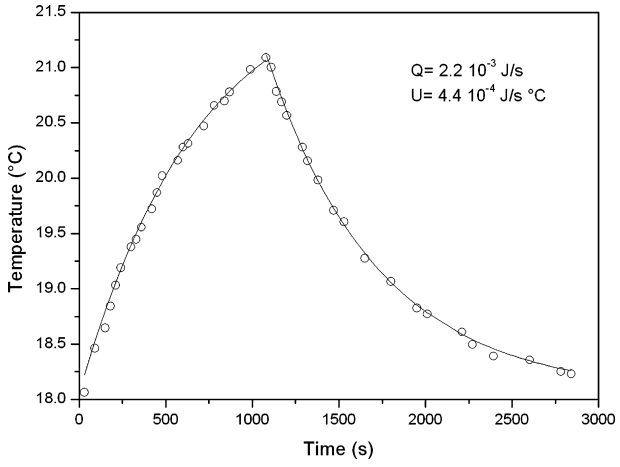

Fig. 5 – Temperature vs. time during irradiation of a 1.5 mm thick monomer sample. The LED unit was turned off at 1200 s.

increase in temperature was 10 and 18 °C. This is consistent with the relative reactivity of the amines because a more reactive amine will lead to a faster polymerization and a faster rate of heat evolution. As described in Section 2, the samples were irradiated for 320 s and the data acquisition continued in the dark to complete 600 s. The discontinuity of the temperature traces at 320 s corresponds to the time at which the LED unit was turned off. It should be noted that the LED may heat the irradiated specimen directly. This thermal heating of the samples by the LED was assessed by monitoring the temperature rise during irradiation of a monomer sample. Fig. 5 shows the recorded temperature values and a theoretical prediction was made as follows. The temperature of the sample for a given time may be calculated from the energy balance which is given by [25]:

$$\rho c_p V \frac{dT}{dt} = q - U'(T - T_0) \quad (\text{Joule/s}) \tag{2}$$

where T is the sample temperature, ρ is the density, c_p is the specific heat, V is the volume, q is the rate of heat generation by the LED init, U' is the global heat transfer coefficient and T_0 is the temperature of the environment. This energy balance assumes that heat transfer within the sample occurs at a higher rate than heat transfer from the sample to the surroundings. This can be predicted by calculating the Biot number for the system, which gives the ratio of internal thermal resistance to external thermal resistance [25]. The Biot number is given by the following relationship: $Bi = hL_c/k$, where h is the heat transfer coefficient evaluated under free convective airflow, k is the thermal conductivity of the resin, and L_c is the thickness of the sample. When this number is small (less than 0.100), the temperature non-uniformity within the sample can be neglected, and it has a spatially uniform temperature that is a function of time only. Estimations of the Biot number for each sample by using conservative values for h and k [k: 0.29 J/m s °C [26], h: 6.7 J/m^2 s [25]) resulted in values lower than 0.1, which validates the use of Eq. (2) for the time evolution of the temperature. Dividing Eq. (2) by $\rho c_p V$:

$$\frac{dT}{dt} = Q - U(T - T_0) \quad (^\circ\text{C/s}) \tag{3}$$

where Q ($q/\rho c_p V$) is the heating rate produced by the LED unit (in °C/s) and U ($U'/\rho c_p V$) is the global heat transfer coefficient per unit volume. Therefore, knowing U and Q makes it possible to assess the influence of the heating by the irradiation source on the sample temperature.

The solution to Eq. (3) is

$$T = T_0 + \frac{Q}{U}(1 - e^{-Ut}) \tag{4}$$

By making Q = 0 in Eq. (3) and integrating:

$$\ln(T - T_0) = -Ut + C_2 \quad \text{and} \quad T - T_0 = (T_i - T_0)\, e^{-Ut} \tag{5}$$

where T_i is the sample temperature when the led was turned off. Then a plot of $\ln(T - T_0)$ versus t, when the LED unit is turned off will give a straight line of slope U. In addition, a plot of $(T - T_0)$ versus $[1 - \exp(-Ut)]$ when the LED is turned on gives a straight line of slope Q/U. By using the U and Q values calculated as described, the temperature versus time was calculated with Eqs. (4) and (5). Fig. 5 shows the computed values along with the experimental measurements. The good agreement between predicted and experimental results lends support to the expressions used for the energy balance. Because the U and Q values depend on the sample volume and cp value, they have to be estimated for each sample. The heating of the led was calculated in 1 and 2 thick samples of monomer and polymer by using the values of ρ and cp of monomer and polymer given in Table 1. Fig. 6 shows the evolution of the sample temperature due to the heating of the LED. It is seen that for 1 and 2 mm thick specimens, the sample heating due to the presence of the LED can be disregarded relative to the curing exotherm and the sample temperature rise may be attributed exclusively to the heat released by the polymerization reaction.

From the results presented in Fig. 4 it emerges that the non-isothermal nature of polymerization will result in volume expansion during heating and this effect will be more marked when the sample thickness increases. Consequently, the volumetric change measured by the device is the combination of contraction due to the polymerization reaction and the expansion or contraction associated with thermal effects.

Table 1 – Density (ρ), heat capacity at 20 °C (cp), and thermal expansion coefficients (α) of the monomer and polymerized samples

Material	ρ (g/cm^3)	cp (J/g K)	α (K^{-1})
Monomer	1.15	1.88	11.8×10^{-4}
Polymer	1.20	1.57	4.5×10^{-4}

The density of the polymer was calculated from the density of the monomer (data sheet from the manufacturer) and the volumetric shrinkage values presented in Fig. 3.

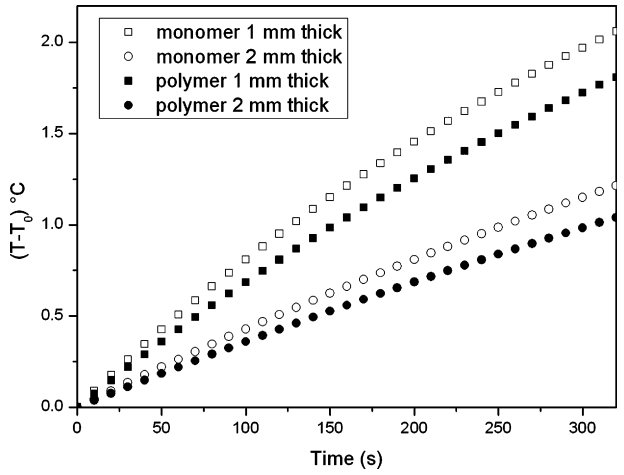

Fig. 6 – Estimation of the heating of 1 and 2 mm thick samples of monomer and polymer by the LED unit. The *U* and Q values for each sample were calculated from the *U* and Q values presented in Fig. 5 and the ρ and *cp* values presented in Table 1.

Volume changes associated with thermal effects are given by:

$$\frac{dV}{V} = \alpha\, dT \quad \text{and} \quad V = V_0\, e^{\alpha\, \Delta T} \tag{6}$$

where α is the volumetric coefficient of thermal expansion, d*V* is the change in the sample volume when the temperature changes by dT and V_0 is the initial sample volume.

The first step for the evaluation of the extent of thermal expansion and contraction is to obtain adequate information of the thermal expansion coefficient of the material. Volumetric changes due to temperature changes are accurately detected by the interferometer, which makes it a suitable technique to measure thermal expansion coefficient. The thermal expansion coefficients of the monomer and vitrified resins are presented in Table 1. To remove the effect of thermal expansion from the overall volume change during cure, the relationship between the volumetric thermal expansion coefficient and the double bond conversion is required. The experimental problem associated with this measurement lies in the fact that the resin polymerizes during heating. Thus, for a first approximation, the thermal expansion coefficient was estimated by the following linear relationship:

$$\alpha = \alpha_m - \frac{x}{x_f}(\alpha_m - \alpha_f) \tag{7}$$

where α_m an α_f are the thermal expansion coefficients of the monomer and the polymer, respectively (Table 1), x is the double bond conversion and x_f is the conversion at the end of the measurement. This expression is similar to that used by Lee and co-workers [27], who studied the volumetric changes during polymerization of unsaturated polyester resins. The conversion versus irradiation time was measured by NIR and the results are shown in Fig. 7. Volumetric changes due to thermal effects were assessed by numerically integrating the discrete values of contraction versus time given by Eq. (6).

$$V = \int \alpha V_0 \frac{dT}{dt} \tag{8}$$

where the time dependence of α was obtained from the conversion-time profiles and Eq. (7). In addition, values of V were calculated as follows:

$$\text{If } V(T) = V_0(T_0)\, e^{\alpha(T-T_0)}$$

$$\text{then} \quad \Delta V_i = V_i - V_{i-1} = V_{i-1}[e^{\alpha i(T_i - T_{i-1})} - 1]$$

where ΔV_i is a discrete change in volume in a time increment between t_{i-1} and t_i, corresponding to temperatures of T_{i-1} and T_i and α_i is calculated from the cumulative change in double bond conversion reached at the time t_i. Thus, the total volumetric shrinkage is:

$$\frac{\Delta V}{V_0} = \frac{1}{V_0}\sum_{1}^{n} V_i(e^{\alpha_i\, \Delta T_i} - 1) \tag{9}$$

Fig. 8 shows the increase and decrease in thickness due to the exothermic effects on expansion and contraction during photopolymerization. It is seen that the theoretically calculated thermal expansion during heating of the sample does not compensate for the thermal contraction of the resin during the cooling period because vitrification occurs during the curing process and, as discussed above, the expansion coefficient in the liquid or gel state is greater than that in the glassy state. After subtraction of the exotherm expansion effect from the overall volumetric changes, the corrected contraction curves are shown in Fig. 9a and b.

The volume shrinkage during polymerization should be related to the number of functional groups that have reacted before the system enters the glassy state. A linear correlation, between volume contraction and mole of converted double bonds, was first proposed in 1953 by Loshaek and Fox [28] and more recent literature [29,30] still refers to this early work. However, plots of volumetric shrinkage measured by

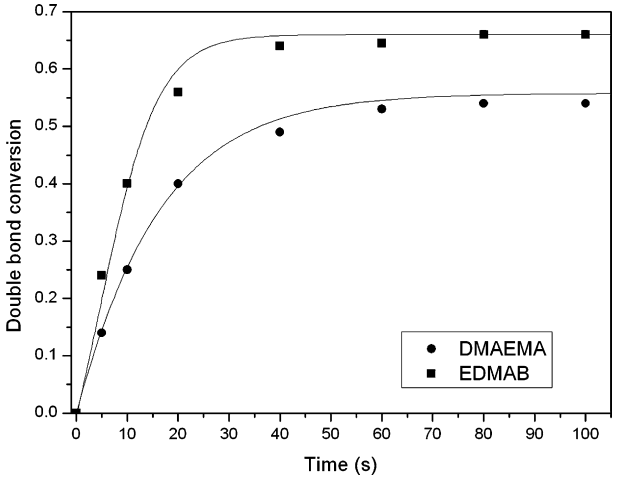

Fig. 7 – Conversion vs. exposure duration measured by NIR for 2 mm thick samples containing 1 wt.% CQ/EDMAB or CQ/EDMAB.

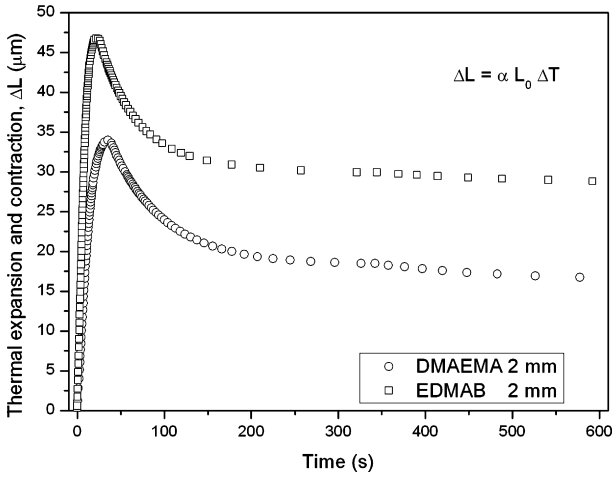

Fig. 8 – Typical plot of change in sample thickness vs. time calculated from Eq. (9) during the photopolymerization of 2 mm thick samples. Computations were made as $\Delta L = \alpha L_0 \Delta T$. Positive values correspond to the heating periods and negative values correspond to the cooling period. The time at which ΔL is maximum corresponds to the time of the maximum rise in temperature (as in Fig. 4). It is seen that the increase in volume during heating is greater than the decrease in volume during cooling.

the interferometer versus double bond conversion measured by NIR are not found to be linear (Fig. 10). This discrepancy could be the result of measuring shrinkage and conversion in different specimen configurations. In order to verify differences between the conversion versus time measured by NIR and shrinkage versus time measured by the interferometer the following measurements were carried out. Samples containing CQ/EDMAB were irradiated for 5, 10, and 20 s and the shrinkage was monitored continuously during and after irradiation. Results of shrinkage evolution presented in Fig. 11 show that a considerable amount of shrinkage took place after the light was turned off. Although no new radicals are generated from initiation when the irradiation is terminated, the remaining free radicals continue to propagate and terminate. As described in Section 2, the acquisition time of the FTIR is 120 s. This means that, due to polymerization in the dark, the conversion versus time measured by FTIR is not equivalent to shrinkage development, which was monitored in a continuous way. Moreover, NIR samples were not open to air, so oxygen inhibition is less important in these measurements. This observation is supported by the different induction times observed for NIR test specimens and shrinkage test specimens. While shrinkage development in the 2 mm thick samples containing the CQ/DMAEMA system was seen only after 8 s, conversions of around 10% were measured by the NIR technique after 5 s irradiation. From these results, it emerges that because of the different data acquisition times between the FTIR and the interferometer, and the different oxygen atmosphere between each test, the double bond conversion and shrinkage measurements are not comparable. An alternative approach was used to correct the experimental curves of contraction. The proposed scheme estimates the polymerization contraction from the experimental shrinkage and temperature profiles shown in Figs. 3 and 4, respectively. The volumetric change measured ($\Delta V_{measured}$) is a combination of contraction due to the polymerization reaction (ΔV_{chem}) and expansion or contraction due to thermal effect (ΔV_{therm}).

$$\Delta V_{measured} = \Delta V_{chem} + \Delta V_{therm} \quad (10)$$

where ΔV_{therm} is positive during heating and negative during cooling. The contraction due to chemical reaction may be expressed in terms of the volume contraction per mole of reactive groups, the number of moles of double bonds per unit mass (which for a blend 70/30 of bis-GMA/TEGDMA is 4.83×10^{-3} mol C=C/g), the density (1.15 g/cm^3) and the double bond conversion, x. Assuming that the reaction of one mole of double bond results in a volumetric contraction equal to 20.4 cm^3 [30] and that the thermal change in volume is given

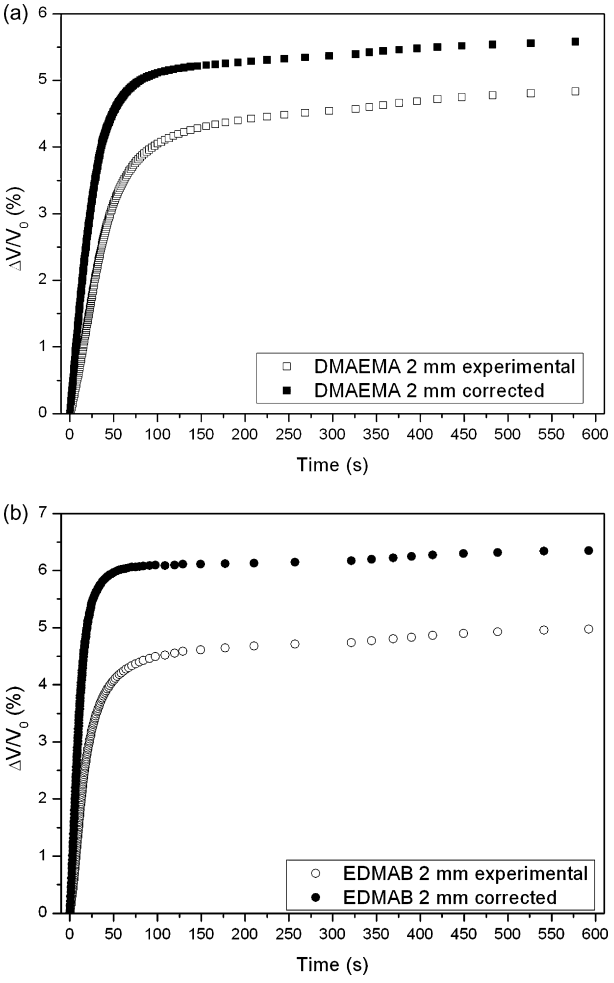

Fig. 9 – (a) Shrinkage profiles corrected with Eq. (8) for 2 mm thick samples of formulations containing 1 wt.% CQ/DMAEMA. The experimental curves are shown for comparison. (b) Shrinkage profiles corrected with Eq. (8) for 2 mm thick samples of formulations containing 1 wt.% CQ/EDMAB. The experimental curves are shown for comparison.

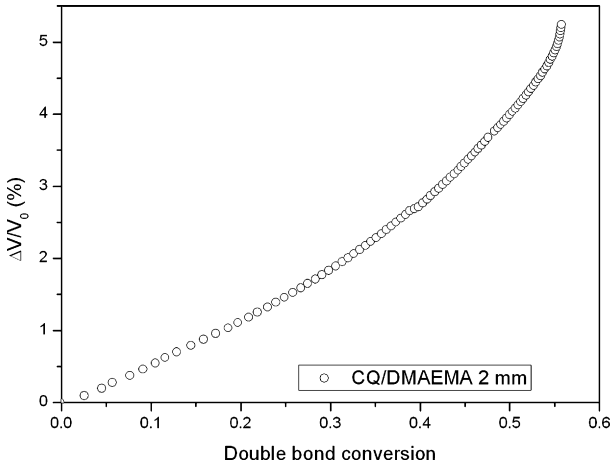

Fig. 10 – Typical plot of corrected shrinkage (from Fig. 9) vs. double bond conversion (from Fig. 7) showing that the values were not fitted by a linear relationship.

from Eq. (9), the overall volume change is given as:

$$\Delta V_{measured} = \left(\frac{V_0}{8.82}\right) x - \left(\alpha_m x - (\alpha_m - \alpha_f)\frac{x}{x_f}\right) V_0 \, \Delta T \qquad (11)$$

In this equation, the double bond conversion, x, and the conversion at the end of the test, x_f, are unknown. Computations were carried out by trial and error assuming an x_u value from which α and x were calculated. The procedure was repeated until the calculated x_f was equal to the assumed x_f value. Figs. 12 and 13 show the predicted conversion profiles and the corrected shrinkage curves calculated, respectively, from Eq. (11). Although the trend in conversion for the different photoinitiator systems is the same as that shown in Fig. 7, the calculated conversion values in the 2 mm thick samples are around 15% lower than that measured by the NIR technique. This is attributed to the exposure of the surface of the specimens in the dilatometric experiments to an air atmosphere which retards the polymerization of the shrinkage samples as compared with the NIR experiments in which the resin was enclosed. In addition, no influence of sample thickness upon double bond conversion (Fig. 13) is predicted. These results are in disagreement with the experimental evidence that the conversion attained by the monomer increases with the cure temperature [22]. Although the difference in the cure temperature between 1 and 2 mm thick samples is not great (Fig. 4), statistically significant differences in double bond conversion and volumetric shrinkage with increasing temperature are expected to occur. In order to explain the trends presented in Figs. 12 and 13, the influence of light attenuation throughout the sample thickness was examined. Photopolymerization

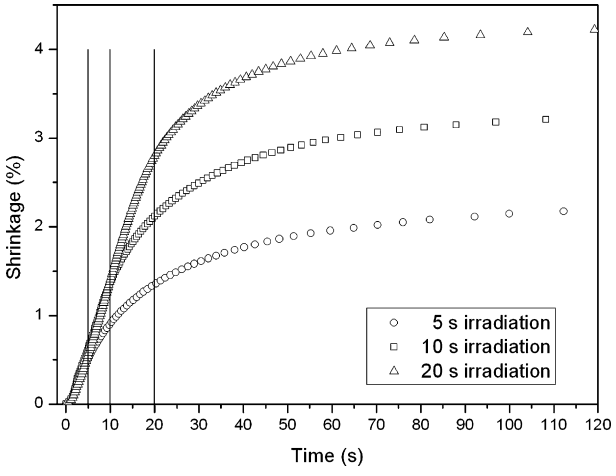

Fig. 11 – Typical plots of shrinkage vs. time of samples irradiated for 5, 10 and 20 s at11.5 mW/cm^2. The shrinkage was monitored during and after exposure to complete 300 s. The lines show the times at which the LED was turned off. Only the first 120 s of test are shown to make the plot clearer. It is seen that a considerable amount of shrinkage took place after the LED was turned off. The sample was 1 mm thick and the formulation was prepared with 1 wt.% CQ/EDMAB.

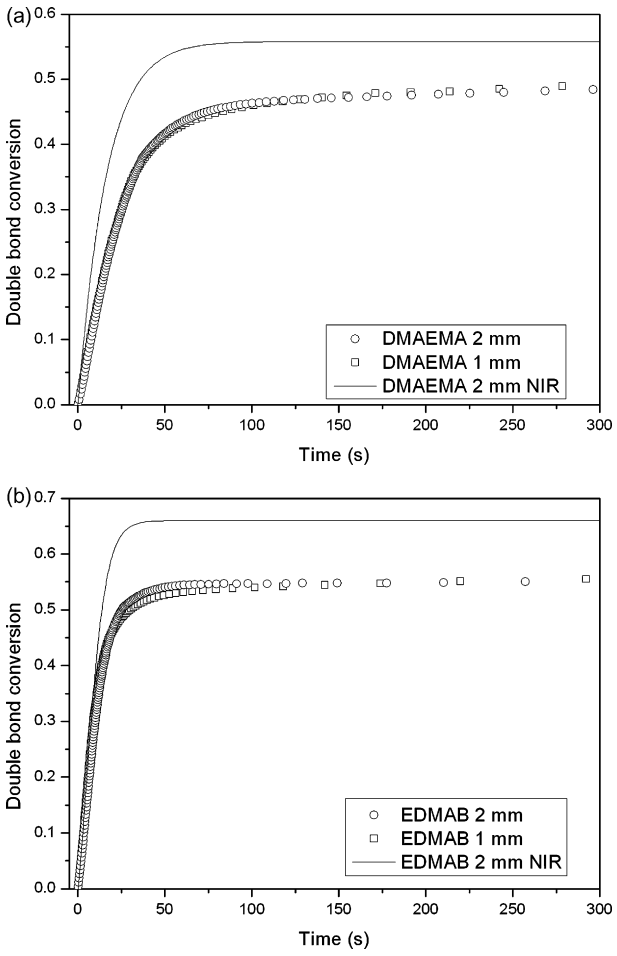

Fig. 12 – (a) Conversion vs. time profiles calculated from Eq. (11) for 1 and 2 mm thick samples containing 1 wt.% CQ/DMAEMA. The conversion measured by NIR in a 2 mm thick sample is shown for comparison. (b) Conversion vs. time profiles calculated from Eq. (11) for 1 and 2 mm thick samples containing 1 wt.% CQ/EDMAB. The conversion measured by NIR in a 2 mm thick sample is shown for comparison.

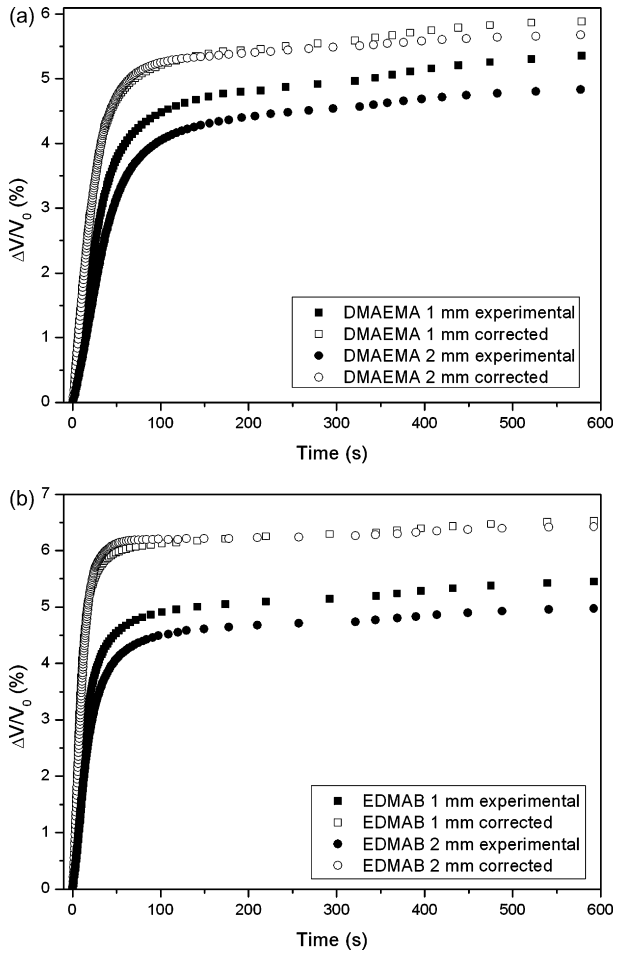

Fig. 13 – (a) Shrinkage profiles corrected by Eq. (11) for formulations containing 1 wt.% CQ/DMAEMA. The experimental curves are also shown for comparison. No influence of sample thickness can be seen in the corrected values. (b) Shrinkage profiles corrected by Eq. (11) for formulations containing 1 wt.% CQ/EDMAB.

in strongly absorbing or thick layers can lead to non-uniform photoinitiation and monomer conversion rates. In fact, the clinically relevant depth of cure of the photocured material, below which no polymerization occurs, is explained in terms of the attenuation of radiation [20,21]. For a non-scattering medium, as is used here, the light intensity decreases along the beam direction according to the Beer–Lambert law, which is given by:

$$A = -\log\frac{I}{I_0} = \varepsilon C l \quad \text{and} \quad I = I_0 10^{(-\varepsilon C l)} \tag{12}$$

Here, A is the absorbance, I_0 is the light intensity at the bottom surface (Fig. 1), I is the light intensity at a depth l into the sample, C is the unreacted initiator concentration, and ε is the molar extinction coefficient of the absorbing species. The extinction coefficient of CQ at a wavelength equal to 467 nm measured by UV–vis spectrophotometry was 43.9 L/mol cm. From this value, the light intensity profiles throughout the sample thickness, was calculated from Eq. (12) and the intensity decay is depicted in Fig. 14. In the 1 mm thick samples the radiation is attenuated by up to 50% across the film thickness whereas in the 2 mm thick specimens the intensity at the top of the sample is 25% of the intensity of the incident light. However during the irradiation process, CQ is photobleached by conversion to moieties transparent or having lower absorption coefficients [31]. Thus, the absorbance of the system decreases and the light beam penetrates deeper as the irradiation time increases, which makes possible the vitrification of thick samples. The kinetics of CQ consumption in bis-GMA/TEGDMA blends (70/30 mass fraction) containing CQ/N,N,3,5-tetramethylaniline (TMA) photoinitiator systems was studied by Cook [31]. UV–vis spectroscopic studies carried out by the author showed that for intermediate to high concentrations of TMA (>0.3 wt.%), the kinetics of the consumption of CQ during irradiation was fitted to a first order expression and that the rate constant was proportional to the radiation intensity but was independent of CQ concentration. UV–vis measurements of decrease of absorbance versus irradiation time at 11.5 mW/cm^2 in samples containing 1 wt.% CQ/amine, showed that under the experimental conditions used, more than 20 min were required to detect a decrease in CQ concentration. This suggests that in samples irradiated for 320 s, the photobleaching of the CQ can be disregarded and the light intensity profile through the path length is the controlling factor that determines the temporal evolution of the polymerization. The rates of primary photochemical processes (e.g. primary free radicals from the photosensitizer) are generally proportional to the product of photoinitiator concentration and local light intensity. Thus, a gradient in polymerization rate, temperature and conversion, is created inside the sample and the temperature and shrinkage values measured by each technique are averaged throughout the sample thickness. The mathematical analysis of the polymerization rate and conversion profiles along the path length is beyond the purpose of the present research which aims to assess the influence of thermal effects on volumetric changes in bulk polymerizing systems. However, from the above analysis it may be concluded that the trends of double bond conversion and shrinkage with

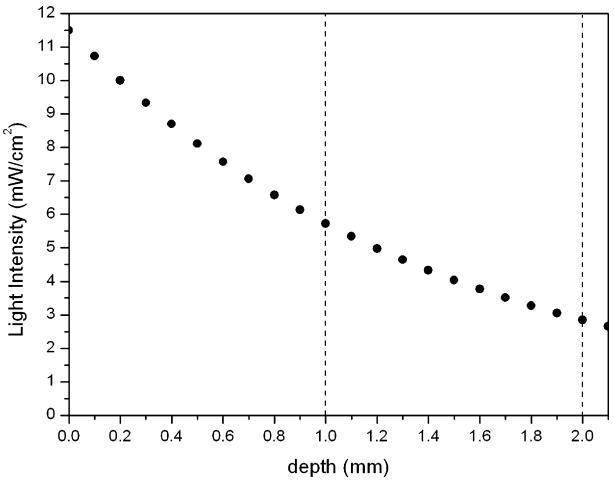

Fig. 14 – Light intensity profile through sample thickness calculated from Eq. (12). The concentration of CQ was assumed unchanged and equal to 1 wt.%.

increased sample thickness (Figs. 12 and 13) can be attributed to the attenuation of the light intensity through the sample thickness. The greater cure temperature of the thicker samples is accompanied by a lower overall light intensity and consequently the degree of double bond conversion averaged through the sample thickness is reduced.

From the results presented it emerges that expansions and contractions due to thermal effects can be easily assessed by measuring the temperature evolution during photopolymerization provided that reliable data of thermal expansion coefficients is available.

4. Conclusions

A novel interferometric method based on a Fizeau-type interferometric scheme was used for monitoring the shrinkage development during photopolymerization of a model unfilled dental resin. The recorded interferograms and the corresponding shrinkage profiles were found to be highly reproducible.

The volumetric change measured during photopolymerization of exothermic systems is a combination of contraction due to the polymerization reaction and expansion or contraction due to the polymerization exotherm and subsequent heat loss to the environment, respectively. The thermal contribution to the overall shrinkage was assessed from the temperature profiles and the thermal expansion coefficients.

Due to the difference in thermal expansion coefficients between the rubbery and glassy resins, the increase in volume due to thermal expansion during the heating of the samples was greater than the decrease in volume during the cooling period. As a result, the resin vitrifies with a volume greater than that calculated from polymerization contraction.

Acknowledgements

The financial support provided by the CONICET and ANPCyT is gratefully acknowledged. The authors are grateful to Esstech for the generous donation of the bis-GMA monomer used in this study.

REFERENCES

[1] Lu H, Stansbury JW, Bowman CN. Towards the elucidation of shrinkage stress development and relaxation in dental composites. Dent Mater 2004;20:979–86.
[2] Lim B-S, Ferracane JL, Sakaguchi RL, Condon JR. Reduction of polymerization contraction stress for dental composites by two-step light-activation. Dent Mater 2002;18:436–44.
[3] Söderholm KJM. Influence of silane treatment and filler fraction on thermal expansion of composite resins. J Dent Res 1984;63:1321–6.
[4] De Gee AJ, Davidson CL, Smith AA. A modified dilatometer for continuous recording of volumetric polymerization shrinkage of composite restorative materials. J Dent 1981;9:36–42.
[5] Reed B, Dickens B, Dickens S, Parry E. Volumetric contraction measured by a computer-controlled mercury dilatometer. J Dent Res 1996;75:2184–92.
[6] Cook WD, Forrest M, Goodwin AA. A simple method for the measurement of polymerization shrinkage in dental composites. Dent Mater 1999;15:447–9.
[7] De Gee AJ, Feilzer AJ, Davidson CL. True linear polymerization shrinkage of unfilled resins and composites determined with a linometer. Dent Mater 1993;9:11–4.
[8] Venhoven BA, De Gee AJ, Davidson CL. Polymerization contraction and conversion of light-curing bisGMA-based methacrylate resins. Biomaterials 1993;14:871–5.
[9] Watts DC, Cash AJ. Determination of polymerization shrinkage kinetics in visible-light-cured materials: methods development. Dent Mater 1991;7:281287.
[10] Sideridou I, Achilias DS, Kyrikou AE. Thermal expansion characteristics of light-cured dental resins and composites. Biomaterials 2004;25:3087–97.
[11] Fogleman E, Kelly M, Grubbs W. Laser interferometric method for measuring linear polymerization shrinkage in light cured dental restoratives. Den Mater 2002;18:324–30.
[12] Fano V, Ortalli I, Pizzi S, Bonanini M. Polymerization shrinkage of microfilled composites determined by laser beam scanning. Biomaterials 1997;18:467–70.
[13] Dudi O, Grubbs W. Laser interferometric technique for measuring polymer cure kinetics. J Appl Polym Sci 1999;74:2133–42.
[14] Arenas G, Noriega C, Vallo C, Duchowicz R. Polymerization shrinkage of a dental resin composite determined by a fiber optic Fizeau interferometer. Opt Commun 2007;271:581–6.
[15] Stansbury J, Dickens S. Determination of double bond conversion in dental resins by near infrared spectroscopy. Dent Mater 2001;17:71–9.
[16] Watts DC, Marouf AS. Optimal specimen geometry in bonded-disk shrinkage-strain measurements on light-cured biomaterials. Dent Mater 2000;16:447–51.
[17] Sakaguchi RL, Wiltbank BD, Shah NC. Critical configuration analysis of four methods for measuring polymerization shrinkage strain of composites. Dent Mater 2004;20:388–96.
[18] Schroeder W, Vallo C. Effect of different photoinitiator systems on conversion profiles of a model unfilled light-cured resin. Dent Mater 2007;23:1313–21.
[19] Schroeder W, Arenas G, Vallo C. Monomer conversion in a light-cured dental resin containing 1-phenyl-1,2-propanedione photosensitizer. Polym Int 2007;56:1099–105.
[20] Cook WD. Kinetics and properties of a photopolymerized dimethacrylate oligomer. J Appl Polym Sci 1991;42:2209–22.
[21] Cook WD. Factors affecting the depth of cure of UV-polymerized composites. J Dent Res 1979;5:800–8.
[22] Cook WD. Thermal aspects of the kinetics of dimethacrylate photopolymerization. Polymer 1992;33:2152–61.
[23] Cook WD. Photopolymerization kinetics of oligo(ethylene oxide) and oligo(methylene) oxide dimethacrylates. J Polym Sci: Part A: Polym Chem 1993;31:1053–67.
[24] O'Brien AK, Bowman CN. Impact of oxygen on photopolymerization kinetics and polymer structure. Macromolecules 2006;39:2501–6.
[25] Bird RB, Stewart WE, Lightfoot EN. Transport phenomena. 2nd ed. New York: John Wiley Sons, Inc.; 2002.
[26] Désilles N, Lecamp L, Lebaudy P, Youssef B, Lebaudy Z, Bunel C. Simulation of conversion profiles within dimethacrylate thick material during photopolymerization. Validation of the simulation by thermal analysis data. Application to the synthesis of a gradient structure material. Polymer 2006;47:193–9.
[27] Hill R, Shailesh J, Muzumdar V, Lee J. Analysis of volumetric changes of unsaturated polyester resins during curing. Polym Eng Sci 1995;35:852–9.
[28] Loshaek S, Fox TG. Cross-linked polymers. I. Factors influencing the efficiency of cross-linking in copolymers of

methylmethacrylate and glycol dimethacrylates. J Am Chem Soc 1953;75:3544–50.
[29] Patel IP, Braden M, Davy K. Polymerization shrinkage of methacrylate esthers. Biomaterials 1987;8:53–6.
[30] Dewaelea M, Truffier-Boutry D, Devauxb J, Leloupa G. Volume contraction in photocured dental resins: the shrinkage–conversion relationship revisited. Biomaterials 2006;22:359–65.
[31] Cook WD. Photopolymerization kinetics of dimethacrylates using the camphorquinone amine initiator system. Polymer 1992;33:600–9.